RESEARCH REPORT

The antifungal activity of a thaumatin-like protein from oyster *Crassostrea gigas*

X Niu[1,3], Q Xu[1,3], W Wang[1,3], Z Yu[1,3], Z Liu[1,3], C Qu[1,3], Y Liu[1,3], C Gong[1,3], L Wang[1,2,3,4], L Song[1,2,3,4*]

[1]*Liaoning Key Laboratory of Marine Animal Immunology, Dalian Ocean University, Dalian 116023, China*
[2]*Laboratory of Marine Fisheries Science and Food Production Processes, Qingdao National Laboratory for Marine Science and Technology, Qingdao 266235, China*
[3]*Liaoning Key Laboratory of Marine Animal Immunology & Disease Control, Dalian Ocean University, Dalian 116023, China*
[4]*Dalian Key Laboratory of Disease Prevention and Control for Aquaculture Animals, Dalian Ocean University, Dalian 116023, China*

Abstract

In the present study, a thaumatin-like protein (*Cg*TLP) was identified from the oyster *Crassostrea gigas*. The full-length cDNA of *Cg*TLP was of 913 bp with a 5' untranslated regions (UTR) of 98 bp, a 3' UTR of 80 bp, and an open reading frame (ORF) of 735 bp encoding a polypeptide of 244 residues. The *Cg*TLP gene was expressed ubiquitously in mantle, gonad, hemocytes, hepatopancreas, gill, and adductor muscle with the higher expression levels in adductor muscle, hemocytes, and hepatopancreas. Immunofluorescence assay indicated that *Cg*TLP was mainly distributed in the cytoplasm of hemocytes. The mRNA expression levels of *Cg*TLP in hemocytes were significantly up-regulated after the stimulations with mannan (13.69-fold, $p < 0.05$), *Pichia pastoris* (8.85-fold, $p < 0.05$) and polyinosinic-polycytidylic acid (3.62-fold, $p < 0.05$), but did not change significantly after stimulations with lipopolysaccharide, peptidoglycan, and *Vibrio splendidus*. The recombinant *Cg*TLP protein (r*Cg*TLP) significantly inhibited the proliferation of *P. pastoris* ($p < 0.05$), while no inhibition towards *Staphylococcus aureus* and *V. splendidus*. r*Cg*TLP also displayed obvious β-1,3-glucanase activity, while no enzymatic activity towards chitin. These results collectively indicated that *Cg*TLP was a homologue of TLP, which might play a vital role in defensing against fungal infection in *C. gigas*.

Key Words: *Crassostrea gigas*; Thaumatin-like protein; Antifungal activity; Immune response

Introduction

Thaumatin was firstly isolated from the seeds of plant *Thaumatococcus danielli* for its exceptionally potent sweet taste (Noh *et al.*, 2016). Subsequently, the proteins with similar amino acid sequences were identified in most of the plant species, which were termed as thaumatin-like proteins (TLPs) (Breiteneder *et al.*, 2000). TLPs are low molecular-weight (20-26 kDa) proteins containing one thaumatin (THN) domain with sixteen conserved cysteine (Cys) residues. The THN domain is peculiar to the thaumatin-like protein family. The Cys form eight intra-molecular disulfide bonds to stabilize the proteins under extreme pH and temperature (Hegde *et al.*, 2014). Most plant TLPs exhibit antifungal activity against a range of pathogenic and nonpathogenic fungi (Cao *et al.*, 2016; Wang *et al.*, 2017), and they are up-regulated in response to a variety of fungal infections and stress (Hegde *et al.*, 2014). Their activities against pathogenic microorganisms are related to the activities of β-1,3-glucanase (Menu-Bouaouiche *et al.*, 2003), glucose polymers depredating (Liu *et al.*, 2010), chitinase (Yasmin *et al.*, 2017), and xylanase (Fierens *et al.*, 2007), as well as α-amylase inhibiting properties (Franco *et al.*, 2002). Meanwhile, TLPs have also been reported in fungi, such as *Irpex lacteus* (Garcia-Casado *et al.*, 2000) and *Cryptococcus neoformans* (Sakamoto *et al.*, 2006) with emphases on gene structure and activities (Blouin *et al.*, 2018). In addition, TLPs have also been reported to exhibit membrane-permeabilizing activity (Meng *et al.*, 2017). However, the detailed mechanisms of their antifungal action are still not completely understood.

With the advances in biological technology and

Corresponding author:
Linsheng Song
Liaoning Key Laboratory of Marine Animal Immunology
Dalian Ocean University
Dalian 116023, China
E-mail: lshsong@dlou.edu.cn

genome information, TLPs have also been found in nematode *Caenorhabditis elegans* (Kitajima *et al.*, 1999), desert locust *Schistocerca gregaria* (Brandazza *et al.*, 2004), Coleoptera *Diaprepes abbreviatus*, Hymenoptera *Lysiphlebus*, and Hemiptera *Toxoptera citricida* (Shatters *et al.*, 2006). For marine animals, the information about TLPs are still very limited, and only the predicted TLPs from *C. gigas* (XP_011414138.1), *Crassostrea virginica* (XP_022333236.1), and *Mizuhopecten yessoensis* (OWF35002.1) have been referred in NCBI (https://www.ncbi.nlm.nih.gov/) based on genomic sequencing.

The Pacific oyster *C. gigas* is one of the most important cultured mollusk species in the world, and it contributes greatly to the economic development of the global aquaculture (Yang *et al.*, 2017). Because of its economic and ecological importance as well as biological characteristics, *C. gigas* is becoming a model to investigate molluscan biology, development, innate immunity, and stress adaptation (Guo *et al.*, 2015). As a sessile marine animal living in estuarine and intertidal regions, *C. gigas* has to face the infections of various pathogens including bacteria, protozoans, fungi, and viruses (Paillard *et al.*, 2004; Guo *et al.*, 2015). Pathogenic fungi, such as *Monilia*, *Ostracoblabe implexa*, *Sirolpidium zoophthorum*, *Dermocystidium marinus*, and *Lagenidium*, can cause more than 95% mortality of the cultured *Crassostrea virginica* in summer (Chen *et al.*, 2007). The characterization of antifungal molecules would benefit the knowledge of the marine animals immune defense mechanism (Franco *et al.*, 2002; Liu *et al.*, 2010; Yasmin *et al.*, 2017). In the present study, a novel homologue of TLP was identified from oysters *C. gigas* (designated as *Cg*TLP). The mRNA expression levels of *Cg*TLP in hemocytes post immune stimulation and its antimicrobial activity were investigated. Moreover, the β-1,3-glucanase and chitinase activities of the recombinant *Cg*TLP protein were detected *in vitro*, which would provide more information to understand the immune defense roles of *Cg*TLP in *C. gigas.*

Materials and methods

Animals, microorganisms, and drugs

Oysters *Crassostrea gigas* with an average shell length of 12.0 cm were sampled from a local farm in Dalian, China, and maintained in aerated seawater at approximately 20 °C and salinity of 30‰ for an acclimation period of seven days. The oysters were fed daily with spirulina powder at a dose of 1-3 g/m^3 water. Six-week-old female mice were purchased from Dalian Medical University (Dalian, China). The bacterium *Staphylococcus aureus* and fungus *Pichia pastoris* were purchased from Microbial Culture Collection Center (Beijing, China) and Invitrogen (Lifetech, USA), respectively. *Vibrio splendidus* was separated from the infected *Patinopecten yessoensis* (Liu *et al., 2013*). The bacteria *V. splendidus* and *S. aureus* were cultured in 2216E media at 28 °C for 20 h and LB media at 37 °C for 20 h, respectively. The fungus *P. pastoris* was cultured in Yeast Extract Peptone Dextrose Medium (YPD) media at 28 °C for 24 h. The cell cultures were harvested by centrifugation and the

pellets were washed with phosphate buffered saline (PBS, 0.14 mol/L NaCl, 3 mmol/L KCl, 8 mmol/L Na$_2$HPO$_4$, 1.5 mmol/L KH$_2$PO$_4$, pH=7.4) for three times, and then re-suspended in PBS at a final concentration of about 1×10^8 CFU/mL. *Escherichia coli* Trans5α (TransGen, China), pET-28a (TaKaRa, Japan) and BL21 (DE3) (TransGen, China) were used for gene cloning and protein expression, respectively. LPS (from *E. coli*, Sigma-Aldrich, USA), PGN (from *S. aureus*, Sigma-Aldrich, USA), Poly (I:C) (Sigma-Aldrich, USA) and MAN (from *Saccharomyces cerevisiae*, Sigma-Aldrich, USA) were dissolved in PBS at a final concentration of 0.5, 1.0, 1.0, and 1.0 mg/mL, respectively.

Immune stimulation and sample collection

For the analysis of *Cg*TLP mRNA distribution, six tissues including gonad, gill, mantle, adductor muscle, hemocytes and hepatopancreas from nine oysters were collected as three parallels. The tissues were kept in Trizol reagent at -80 °C for RNA extraction.

Four hundred and twenty oysters were randomly selected and separated into seven groups for fungus, bacteria and pathogen associated molecular patterns (PAMPs) stimulations to reveal the mRNA expression of *Cg*TLP. Fungus *P. pastoris*, bacterium *V. splendidus* and four different PAMPs were used for immune stimulations. The oysters in the treatment groups (80 oysters in each group) individually received an injection of 100 μL live *V. splendidus* (1×10^8 CFU/mL in PBS), *P. pastoris* (1×10^8 CFU/mL in PBS), LPS, PGN, Poly (I:C) and MAN, respectively. The LPS, PGN, Poly (I:C) and MAN were prepared at the concentration of 0.5, 1.0, 1.0, and 1.0 mg/mL in PBS as described above, respectively. The rest oysters in the control group received an injection of 100 μL PBS. Nine oysters were randomly sampled from each group at 0, 3, 6, 12, 24, 48 and 72 h after injection and divided into three parallels. The hemolymphs collected from three oysters were pooled together as one sample. There were three parallels for each time point. The hemocytes were kept in Trizol reagent at -80 °C for RNA extraction.

RNA isolation and cDNA synthesis

The total RNA was obtained from tissues using Trizol reagent according to the manufacture's protocol (Invitrogen, USA) and quantified by Nanodrop 2000 (Thermo Scientific, USA). The first strand cDNA was reverse-transcribed based on manufacture's protocol using the PrimeScript^{TM} 1st Strand cDNA Synthesis Kit (TaKaRa, Japan). The cDNA mix was diluted 50-fold and stored at -80 °C for subsequent SYBR Green fluorescent quantitative real-time PCR (qRT-PCR).

The gene cloning of Cg*TLP*

The DNA fragment of *Cg*TLP (GenBank accession No. XM_011415836.2) (Zhang *et al.*, 2012) was amplified using ExTaq DNA polymerase (TaKaRa, Japan). The information of the primers used in this study was listed in Table 1. The PCR products were cloned into the pMD19-T (TaKaRa, Japan) and verified by nucleotide sequencing in both directions.

Table 1 Primers used in this study

Primer purpose	Primer name	Sequence (5'-3')
Clone primers	*Cg*TLP-5'-F	TTAACATTTGGAGATAAAGAACT
	*Cg*TLP-3'-R	TGAAAGTATTTCAACAAATTGTAAT
	*Cg*TLP-ORF-F	ATGAACAAGATAGCCATGAAGT
	*Cg*TLP-ORF-R	TTATCCACAGAAGACGACATC
qRT primers	*Cg*TLP-qRT-F	GAAGGGCAATCGGGAGCATA
	*Cg*TLP-qRT-R	GGGCGTATGAGAAGTTTGGA
	*Cg*EF-qRT-F	CTCCACCCAACATCACCACT
	*Cg*EF-qRT-R	GGATTTCCTTTACGGACACG
Recombination primers	*Cg*TLP-recombinant-F	GGAATTCCATATGCACAGAATCCATTATAGAAAC
	*Cg*TLP-recombinant-R	CCGCTCGAGTCCACAGAAGACGACATC

Bioinformatics analysis of Cg*TLP*

The amino acid sequence of *Cg*TLP was analyzed using the Sequence Manipulation Suite (http://www.bio-soft.net/sms/), and domains were predicted by using the simple modular architecture research tool (SMART) (http://smart.embl-heidelberg.de/). The three-dimensional models of TLPs were built by homology modeling with the SWISS-MODEL prediction algorithm (http://swissmodel.expasy.org/). The amino acid sequences of TLPs from other species were obtained from NCBI (https://www.ncbi.nlm.nih.gov/) database. The Clustal x1.81 and the Sequence Manipulation Suite (http://www.bio-soft.net/sms/) were used to perform the multiple sequence alignment for TLPs. A phylogenetic tree was constructed by the neighbor joining (NJ) method using the software of MEGA 6.06. The reliability of the branching was tested by using bootstrap re-sampling (1000 pseudo-replicates).

Quantitative real time PCR analysis (qRT-PCR) of the mRNA expression

The relative mRNA expression levels of *Cg*TLP were measured by SYBR Green fluorescent qRT-PCR, which was performed with an ABI 7500 Real-time Thermal Cycler (Applied Biosystems, USA) according to the manufacture's instruction with SYBR Premix Ex Taq (Tli RNaseH Plus) (TaKaRa, RR420A). A pair of specific primers, *Cg*TLP-qRT-F and *Cg*TLP-qRT-R (Table 1), was used to amplify a fragment of 202 bp. The *C. gigas* elongation factor (*Cg*EF, NM_001305313.2) fragment amplified with primers *Cg*EF-qRT-F and *Cg*EF-qRT-R (Table 1) was employed as the internal control (Zhang *et al.*, 2012). The mantle and the time of 0 h were used as the reference group, respectively. The mRNA expression levels of *Cg*TLP were determined by $2^{-\Delta\Delta Ct}$ method (Livak *et al.*, 2001). All the data were given in terms of relative mRNA expression as mean ± S.D. (N=3).

The expression and purification of recombinant Cg*TLP*

The ORF fragment of *Cg*TLP without signal peptide sequence was cloned with primers *Cg*TLP-recombinant-F and *Cg*TLP-recombinant-R (Table 1) with an *Nde* I and *Xho* I site at their 5' end, respectively. After cloned into pMD19-T simple vector (TaKaRa, Japan) and transformed into *E. coli* Trans5α, the target fragment was obtained by completely digestion with restrictive enzymes *Nde* I and *Xho* I, and subsequently cloned into the *Nde* I/*Xho* I sites of expression vector pET-28a (Novagen, USA). The recombinant plasmids pET-28a-*Cg*TLP were transformed into *E. coli* BL21 (DE3) (TransGen, China) for prokaryotic expression of *Cg*TLP. The recombinant proteins of *Cg*TLP (r*Cg*TLP) were purified by Ni^{2+} chelating sepharose column (Sangon Biotech, Canada) and dialysed with the dialysate. The purified r*Cg*TLP was examined by 15% SDS-PAGE, and visualized with Coomassie Bright Blue R250. The purified protein was quantified by Bradford Protein Assay Kit (Beyotime, China) and stored at -80 °C.

Preparation of polyclonal antibodies, western blotting, and subcellular localization of Cg*TLP in hemocytes*

Three six-week-old female mice were immunized with r*Cg*TLP protein to generate polyclonal antibody as the method described in the previous report (Sun *et al.*, 2014). In short, 300 μL of recombinant protein (about 200 μg) was mixed with an equal volume of Freund's complete adjuvant, and injected into the abdomen of mice. Two weeks later, three immunizations were conducted weekly with an equal volume of Freund's incomplete adjuvant. One week after the fourth immunization, the serum was collected.

r*Cg*TLP was electrophoretically transferred onto a piece of nitrocellulose transfer membrane after a 15% SDS-PAGE. After blocked in TBS-T (10 mM Tris-HCl, pH 8.0, 100 mM NaCl and 0.05% Tween

20) containing 5% skim milk powder at 37 °C for two hours, the membrane was incubated with antiserum solution (1:1000, v/v) at room temperature (RT) for one hour, washed three times with TBS-T, and then incubated with HRP-labeled anti-mouse IgG 1:2000 (v/v) at RT for one hour. After three times washing with TBS-T, the membrane was incubated with ECL detection reagents (Amersham Biosciences, USA) and exposed to film after the final washing with TBS-T for three times.

The hemolymph was collected from healthy oysters with the equal volume of anti-aggregation solution (Zhang *et al.*, 2014). After washed with sterile seawater for three times, the hemocytes were seeded into cell culture dishes (NEST, USA), and incubated in a humidifying box at RT for one hour. The hemocytes were fixed by 4% paraformaldehyde for 20 minutes, and treated with 0.5% Triton X-100 (prepared with PBS) for 20 minutes to permeabilize the cell membrane. After washed with PBS-T for three times, the samples were blocked with 20 μL of 3% BSA at RT for 30 minutes, and then incubated with polyclonal antibody of r*Cg*TLP diluted with 3% BSA in the ratio of 1:500 at 37 °C for one hour. The hemocytes were incubated with Alexa Fluer® 488 (Life technologies, USA) labeled rabbit anti-rat secondary antibody (1:1000) at 37 °C for 30 minutes. Then 4',6-diamidino-2-phenylindole (DAPI, Beyotime Biotechnology, China) was added at the ratio of 1:1000 and incubated for five minutes to dye the nucleus. After washed three times with TBS-T, hemocytes were observed with an LSM 710 laser confocal scanning microscope (Carl Zeiss Jena, Germany).

The assay of microbe growth suppression activity of r*Cg*TLP

The antimicrobial activities of r*Cg*TLP against gram-positive bacterium (*S. aureus*), gram-negative bacterium (*V. splendidus*) and fungus (*P. pastoris*) were determined according to the method described in previous report (Li *et al.*, 2015). *S. aureus*, *V. splendidus* and *P. pastoris* were grown in LB medium 37 °C for 20 hours, 2216E medium 28 °C for 20 hours, YPD medium 28 °C for 24 hours to mid-logarithmic phase, respectively. The cultures were centrifuged at 800 *g*, 4 °C for 10 minutes, and the microorganism pellets were re-suspended with accordingly medium at the concentration 10^5 CFU/mL. Fifty microliter of gradient diluent r*Cg*TLP (protein concentrations at 0.500 mg/mL, 0.250 mg/mL, 0.125 mg/mL, and 0.000 mg/mL in PBS, respectively), 50 μL microorganism resuspension, and 1000 μL of accordingly medium were added into a 96-well microliter plate, respectively, and the plates were placed in an ELISA reader at 28 °C with a shake uninterruptedly. OD_{600} was measured every one hour to detect the growth of bacteria and fungi. Accordingly mediums were used as blank controls. There were three replicates for each group.

The β-1,3-glucanase and chitinase activities assays of r*Cg*TLP

The β-1,3-glucanase activity was measured with a β-1,3-glucanase (β-1,3-GA) Assay Kit (BC0360, Solarbio, China). Briefly, 100 μL of reagent 1 was added to 100 μL r*Cg*TLP (protein concentrations

were 0.500 mg/mL) in a centrifuge tube. The same volume of distilled water was employed as negative control. After incubated at 37 °C for one hour, 600 μL of reagent 2 were appended to the tube and incubated at 100 °C for five minutes. Two hundred microliter of reaction mixture was added to a 96-well microliter plate, which was measured absorbance at 540 nm in an ELISA reader. Each experiment was repeated in triplicate.

The chitinase activity of r*Cg*TLP was measured with a Chitinase Assay Kit (BC0820, Solarbio, China) according to the instruction. In brief, 200 μL extracting solution and 400 μL reagent 1 was added to 400 μL r*Cg*TLP (protein concentrations were 0.500 mg/mL), and 600 μL extracting solution was added to 400 μL r*Cg*TLP (protein concentrations were 0.500 mg/mL) in a centrifuge tube as negative control. The tube was incubated at 37 °C for one hour followed by centrifugation at 5000 rpm, 4 °C for ten minutes. Two hundred microliter of reagent 2 was added to the reaction mixture followed by incubation at 100 °C for seven minutes. Two hundred microliter of reagent 3 and 400 μL of reagent 4 were added to the tube followed by incubated at 37 °C for 15 minutes. Two hundred microlitre reaction mixture was added to a 96-well microliter plate, and the absorbance at 585 nm was measured in an ELISA reader. Each experiment was repeated in triplicate.

Statistical analysis

The data were analyzed by using SPSS 18.0 and expressed as means ± standard deviation (N=3). The statistically significant differences among groups were designated at $p < 0.05$ by one-way analysis of variance (ANOVA) (labeled with *).

Results

The molecular feature, domain and spatial structure of Cg*TLP*

The coding sequence of *Cg*TLP was retrieved from NCBI (XM_011415836.2). The complete cDNA of *Cg*TLP was of 913 with a 98 bp 5' untranslated regions (UTR), an 80 bp 3' UTR and an open reading frame (ORF) of 735 bp (Fig. 1A). The ORF encoded a putative polypeptide of 244 amino acid residues with a predicted molecular weight of 25.97 kDa and theoretical isoelectric point of 7.84. There was a signal peptide (from M^1 to G^{20}) in the deduced amino acid sequence of *Cg*TLP, and a classic SMART THN domain of TLP protein family from I^{23} to G^{244} (Fig. 1A and Fig. 1B). In the spatial structure of *Cg*TLP, there were three domains and a cleft structure. Domain Ⅰ was formed by a β-sandwich with 11 β-sheets, domain Ⅱ was made up by one β-sheet, and domain Ⅲ was composed of three α-helical structures. The cleft structure was localized between domains Ⅰ and Ⅱ (Fig. 1C).

The phylogeny of Cg*TLP*

Multiple sequence alignment was performed on the basis of the deduced amino acid sequences of *Cg*TLP and some other TLPs downloaded from NCBI. The deduced amino acid sequence of *Cg*TLP shared higher similarity with TLPs from other organisms, such as 94% similarity with thaumatin-like
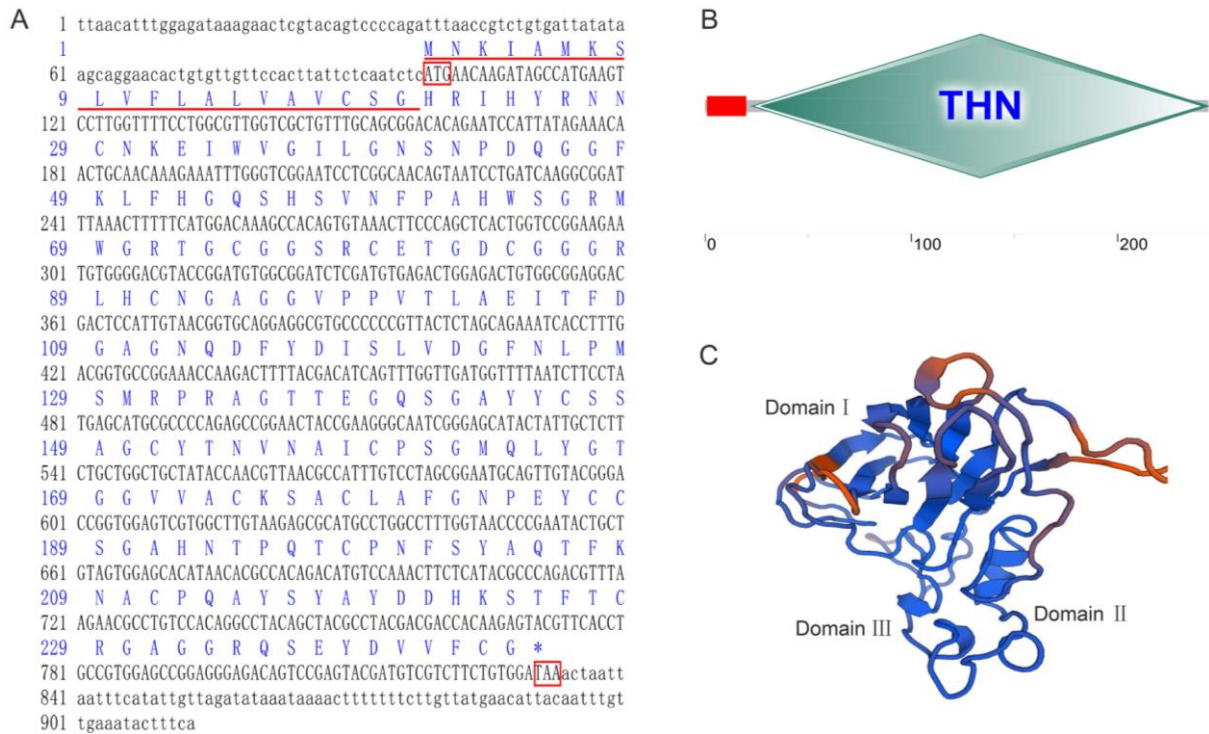
Fig. 1 The molecular feature, domain and spatial structure of *Cg*TLP. A: The cDNA and amino acid sequences of gene encoding *Cg*TLP from *C. gigas*. The nucleotides and amino acids were numbered along the left margin. The putative signal peptide was underlined. The initiation codon and termination codon were boxed in red. B: The structural domain of *Cg*TLP predicted by SMART. The red area represented the signal peptide. C: The spatial structure of *Cg*TLP predicted by SWISS-MODEL program

protein from *C. virginica* (XP_022333236.1), 51% similarity with pathogenesis-related protein 5 like protein from *M. yessoensis* (XP_021343380.1), 49% similarity with *Arabidopsis thaliana* pathogenesis-related protein 5 (NP_177641.1) and 37% similarity with *Rhizoctonia solani 123E* pathogenesis-related protein PR5K (KEP50242.1), respectively (Fig. 2). In the phylogenic tree, 28 TLP proteins from *C. elegans*, *S. gregaria*, *Aleuroglyphus ovatus*, *M. yessoensis*, *A. thaliana* and *R. solani 123E et al.* were gathered separately as three major distinct branches including fungi, Plantae, and animalia. There were three distinct clades in the branch of animalia, nemathelminthes, molluscs and arthropods. *Cg*TLP was firstly clustered with TLP from *C. virginica* and PR-5 from *M. yessoensis* to form molluscan branch, which was a sister branch to nemathelminthes and arthropods (Fig. 3).

The distribution of CgTLP in different tissues

The mRNA transcripts of *Cg*TLP were detected in all the examined tissues, including mantle, gonad, hepatopancreas, hemocytes, adductor muscle, and gill (Fig. 4). The highest mRNA expression level of *Cg*TLP was detected in adductor muscle, which was 64.88-fold ($p < 0.05$) of that in mantle. The mRNA expression levels of *Cg*TLP in hepatopancreas (45.64-fold, $p < 0.05$)and hemocytes were also significantly higher (34.58-fold, $p < 0.05$) than that in mantle, respectively. Nevertheless, the mRNA

expression levels of *Cg*TLP were relatively lower in gonad and gill, which were 2.46-fold ($p < 0.05$) and 1.13-fold ($p > 0.05$) of that in mantle, respectively (Fig. 4).

The mRNA expression pattern of CgTLP in hemocytes after different immune stimulations

The temporal mRNA expression of *Cg*TLP in oyster hemocytes was examined at 0, 3, 6, 12, 24, 48 and 72 h after LPS, PGN, Poly (I:C), or MAN stimulation, respectively. Compared with PBS control group, the mRNA expression level of *Cg*TLP in hemocytes was significantly increased at 12 h (6.56-fold, $p < 0.05$), maintained higher levels from 24 h to 48 h, and then peaked at 72 h (13.69-fold, $p < 0.05$) after MAN stimulation. The mRNA expression level of *Cg*TLP in hemocytes was significantly up-regulated to the peak level at 6 h (3.62-fold of the control group, $p < 0.05$) and then recovered to the original level at 12-72 h ($p > 0.05$) after Poly (I:C) stimulation (Fig. 5A). However, there was no significant change of *Cg*TLP mRNA expression in hemocytes after LPS or PGN stimulation ($p > 0.05$) (Fig. 5A).

The temporal change of *Cg*TLP mRNA expression levels in hemocytes were also monitored after live *V. splendidus* or *P. pastoris* stimulation. The mRNA expression of *Cg*TLP in hemocytes was significantly up-regulated to 5.45-fold ($p < 0.05$) at 12 h post *P. pastoris* challenge, and then continuously

```
Crassostrea gigas        - - - m n k i a m k s l v f l a l v a v c s g h r i h y r n n c n k e i w v g i l g n s - - - n p d q g g f k l f h g q   54
Crassostrea virginica    - - - - - - - m k t l v v l a l v a i c n g h r i h y r n n c n k e i w v g i l g n s - - - i p d q g g f k l f h g q   49
Mizuhopecten yessoensis  - - - - - m l a s l t l l v s a a t v c l a d h t f h v e n h c s y t v w a a a y g n n g - q t p l g g g w e m r a g a   54
Schistocerca gregaria    - - - m i t v a h s l l v a v a s l s e g r t f q f q n k y g e t i w v g s l g n p g h q s i n g g g w e m a a g s   56
Acyrthosiphon pisum      - - - - - m d f k f i l f f v q t a a i t m a h v i t i k n n c p f t i w p g i q g n p g h g h l e n g g f s l g a h k   55
Caenorhabditis briggsae  - - - m i l v k l t v p f f l f a v a a e s r n i t i y n r e p f t i w p g i l g - p g n p - - a g g g f k l d a g q   53
Arabidopsis thaliana     m a n l l v s - t f i f s a l l l i s t a t a a t f e i l n q c s y t v w a a - - - - - a s p g g g r r l d a g q   51
Theobroma cacao          m s s f k t l p t l s f l f v t l f s l a h a a t f d i r n n c p y t v w a a - - - - - - - a v p g g g r p m n r g e   52
Rhodotorula              - - - - m l y l v s t l l s l a a s l v a a q r q f e i i n n c a e t l w p a r p e y l r - - s y t g l r g w m a p p g   54
Folsomia candida         - - - - - - - m k v l l l l c f v a f a h s r q i s f t n r c s q d v w v s p l t n a q g p p h p d g i r r l a n g a   52

Crassostrea gigas        s h s v n f p a h w - s g r m w g r t g c - - - - g g s - r c e t g d c g g g r l h c n g a g g v p p v t l a c i t f d   108
Crassostrea virginica    s h s v n f p s h w - s g r m w g r t g c - - - - g g s - r c e t g d c g g g r l h c s g a g g v p p v t l a c i t f d   103
Mizuhopecten yessoensis  r r s f t v v d h w - n g r i w g r t h c - - - - t g s g q c q t g d c g g - i q c n g r t g r p p a t l a c f t l d   107
Schistocerca gregaria    t m t v n v d d s w - q g r i w g r t c g c k f d a s g r g s c q t g d c g g - v l k c n g a g g k p p s s l l c v t l r   114
Acyrthosiphon pisum      t h t i n t s r d w - a g r i w g r t k c - - - - s a q g k c e t g d c g n - k i k c n g a g g v p p v s l a c m t f t   109
Caenorhabditis briggsae  s r n i n v d d a w t a g i i w a r t t c - - - - d g n f n c e t g f c r n - s e q c n g a g g v p p a s l a c f t l k   108
Arabidopsis thaliana     s w r l d v a a g t k m a r i w g r t n c n f d s s g r g r c q t g d c s g - g l q c t g w g q - p p n t l a c y a l n   109
Theobroma cacao          t w q i s a a p g t t q a r i w a r t n c q f d a s g r g k c q t g d c g g - v l c c k g y g s - p p n t l a c y a i g   110
Rhodotorula              h r q t l v l p e n w n g r i w p r r k c n f t p y g q g t c v t g n c a s - g l n c q d h e g - d f f s l g c f n l n   112
Folsomia candida         t h v y q i s d a g w g g r f w p k t g c d - - - a n g q n c e v g q s v d p c l p t g - - c d p p a c t k v c f f f p   107

Crassostrea gigas        g a g n q d - - f y d i s l v d g f n l p m s m r p r a g t t e g - q s g a y y c s s a g c y t n v n a i c p s g - -   162
Crassostrea virginica    g a g n q d - - f y d i s l v d g f n l p m s m r p r g g t t e g - a s g a y y c t s a g c y t d i n h i c p s g - - -   157
Mizuhopecten yessoensis  g w g g e d - - f y d l s l v d g f n i m m t i q p v a g s y d t n h h g q y y c a r a g c y t d l n q q c p g e q - -   163
Schistocerca gregaria    g s g g n d - - y y d v s l v d g y n l p i t m t p - t d a s g g d - - h y r c r p a t c t a n v n a k c p s e l - -   167
Acyrthosiphon pisum      g s g g l d - - f y d v s l v d g y n l p i r m l p - t g q f s y t k k g k y d c k a a g c v a d l n s m c p s e l - -   164
Caenorhabditis briggsae  s w g g p d - - l y d v s l e d g y n i p v l i e p - h g g s g c k r - - - - - - a g g c v k d i n s e c p e a l - -   156
Arabidopsis thaliana     q f n n l d - - f y d i s l v d g f n i p m e f s p t s s n c h r i l - - - - - - - - - c t a d i n g q c p - - - -   152
Theobroma cacao          q f a n q d - - f i d i s n i d g f n v p m e f s s n s p g c t r v i k - - - - - - - - - c t a d i v g q c p - - - -   154
Rhodotorula              s w g s l d - - f y d l s f v a g f d v p m s i a p a g - - - c q e l a - - - - - - - - - c a s d m t r l c p d e r m k   158
Folsomia candida         p i t n t d d v w y d v s l v d g y s l p a q i i p d q n g g a c v p t - - - - - - - - - h c a v s l d a c p q n d l e   158

Crassostrea gigas        - - - m q l y g t g g v a c k s a c l a f g n p e - - - - - - - - - - - - - - - y c c s g a h n t p q t c p n - f s y   203
Crassostrea virginica    - - - m q l y g t g g v a c k s a c l a f g n p e - - - - - - - - - - - - - - - y c c s g a h n t p q t c p n - f s y   198
Mizuhopecten yessoensis  - - - r q i y g - g q v i a c k s a c e a t g r d d - - - - - - - - - - - - - - - y c c r n a h n t p q t c p s - f p g   203
Schistocerca gregaria    - - - q v v a n - g a v v a c k s a c l a f n t d - - - - - - - - - - - - - - - y c c r g a y n t p q t c k s - s t w   207
Acyrthosiphon pisum      - - - a v k t g - s g v v a c k s a c e r f n t d t - - - - - - - - - - - - - - - y c c r g a h k t p a t c k s - s s w   204
Caenorhabditis briggsae  - - - s v k g h n g y t v a c k s g c l g y n t d q - - - - - - - - - - - - - - - e c c r g a y g t p e k c h r - s a t   197
Arabidopsis thaliana     - - - - - - n v l r a p g g c n n p c t v f q t n q - - - - - - - - - - - - - - - y c c t n q q g c s c s d t v - - - -   186
Theobroma cacao          - - - - - n e l k v p g g c n g p c p v f k t c e - - - - - - - - - - - - - - - h c c n s - - g n c g p t n - - - - -   186
Rhodotorula              q r d a s g n v v g c r s a c f a g i n a e v p s m - - - - - - - - - - - - - - - n c c s g i y e s i p a c v p - e - -   200
Folsomia candida         v g d l r v i k n g r t v a c l a p c k k w n y p p p f g h g r p e d i c p g l w l c c p t p p i d p l a c r a g l v v   218

Crassostrea gigas        a q - - - - t f k n a c p q a y s y a y d d - - - - h k s t f t c r g a g g r q s e y d v v f c g - - - - - - - - - -   244
Crassostrea virginica    a q - - - - t f k n a c p q a y s y a y d d - - - - h k s t f t c r g a g g r q s e y d v i f c g - - - - - - - - - -   239
Mizuhopecten yessoensis  a d - - - - f f k s r c p e a y s y a y d d - - - - h k s t f t c r - - g n p k t a y t v r f c - - - - - - - - - -   241
Schistocerca gregaria    p k n y p s f f k g l c p d a y s y a y d d - - - - k s s t f t c a - - n - - - t g y r i t f g - - - - - - - - - -   246
Acyrthosiphon pisum      p k n y p a f f k k a c p d a y s y a y d d - - - - t t s t f t c r - - g n p s t k y d v i f c p - - - - - - - - - -   247
Caenorhabditis briggsae  d q - - - - m f k d a c p t v y t y r f d d - - - - p s s t f t c q - - s - - k a s y t v q f c - - - - - - - - - -   233
Arabidopsis thaliana     - - - y s r f f k q r c p d a y s y p q d d - - - - p s t f t c t n - - - - - t n y r v v f c p r - - s r l g a t g s   232
Theobroma cacao          - - - f s k f f k d r c p d a y s y p k d d - - - - p t s l f t c p t g - - - - t n y k v i f c p - - - - - - - - - -   224
Rhodotorula              r v d y y n v f k p i c p n a f w y p r d q r d g h p q v d w a c p a g n - - k p k y t i t f c p i g g a k i g s k n i   258
Folsomia candida         r t a y v d l v h r t c p s a y s y s y d d - - - - e a g l h n c p t - - - - n t n f a v t f c p - - - - - - - - - -   259

Crassostrea gigas        - - - - - - - - - - - - - - - - - - - - -   244
Crassostrea virginica    - - - - - - - - - - - - - - - - - - - - -   239
Mizuhopecten yessoensis  - - - - - - - - - - - - - - - - - - - - -   241
Schistocerca gregaria    - - - - - - - - - - - - - - - - - - - - -   246
Acyrthosiphon pisum      - - - - - - - - - - - - - - - - - - - - -   247
Caenorhabditis briggsae  - - - - - - - - - - - - - - - - - - - - -   233
Arabidopsis thaliana     h q l p i k m v t e e n - - - - - - - - -   244
Theobroma cacao          - - - - - - - - - - - - - - - - - - - - -   224
Rhodotorula              g e s l s t f a s s t t p r s r s g e d   278
Folsomia candida         - - - - - - - - - - - - - - - - - - - - -   259
```

Fig. 2 Multiple alignment of *Cg*TLP with other TLP family proteins deposited in GenBank. The same amino acids were shaded in dark and similar amino acids were shaded in grey. Species and gene accession numbers are as follows: *Crassostrea gigas* (XP_011414138.1), *Crassostrea virginica* (XP_022333236.1), *Mizuhopecten yessoensis* (OWF35002.1), *Schistocerca gregaria* (AAR97603.1), *Acyrthosiphon pisum* (NP_001313585.1), *Caenorhabditis briggsae* (CAP30301.1), *Arabidopsis thaliana* (CAA61411.1), *Theobroma cacao* (EOY24665.1), *Rhodotorula* (KWU43254.1), and *Folsomia candida* (XP_021955579.1)

increased to the peak level at 72 h (8.85-fold, $p < 0.05$) (Fig. 5B). There was no significant change of *Cg*TLP expression ($p > 0.05$) after the injection of *V. splendidus* during the whole experimental process (Fig. 5B).

The polyclonal antibody of Cg*TLP and its subcellular localization in hemocytes*

The recombinant plasmid pET-28a-*Cg*TLP was transformed and expressed in *E. coli* BL21 (DE3). After Isopropyl β-D-Thiogalactoside (IPTG) induction, the whole cell lysate was analyzed by 15%

SDS-PAGE, and an obvious band about 25.0 kDa was observed (Fig. 6A). The band was highly consistent with the predicted molecular mass (25.97 kDa) of *Cg*TLP. The purified r*Cg*TLP was injected into the mice to obtain the immune serums. A clear primary reaction band was revealed by western blotting assay, indicating the high recognition specificity of the polyclonal antibody against *Cg*TLP (Fig. 6B).

The localization of *Cg*TLP protein in the hemocytes was analyzed by immunofluorescence assay with the polyclonal antibody acquired from
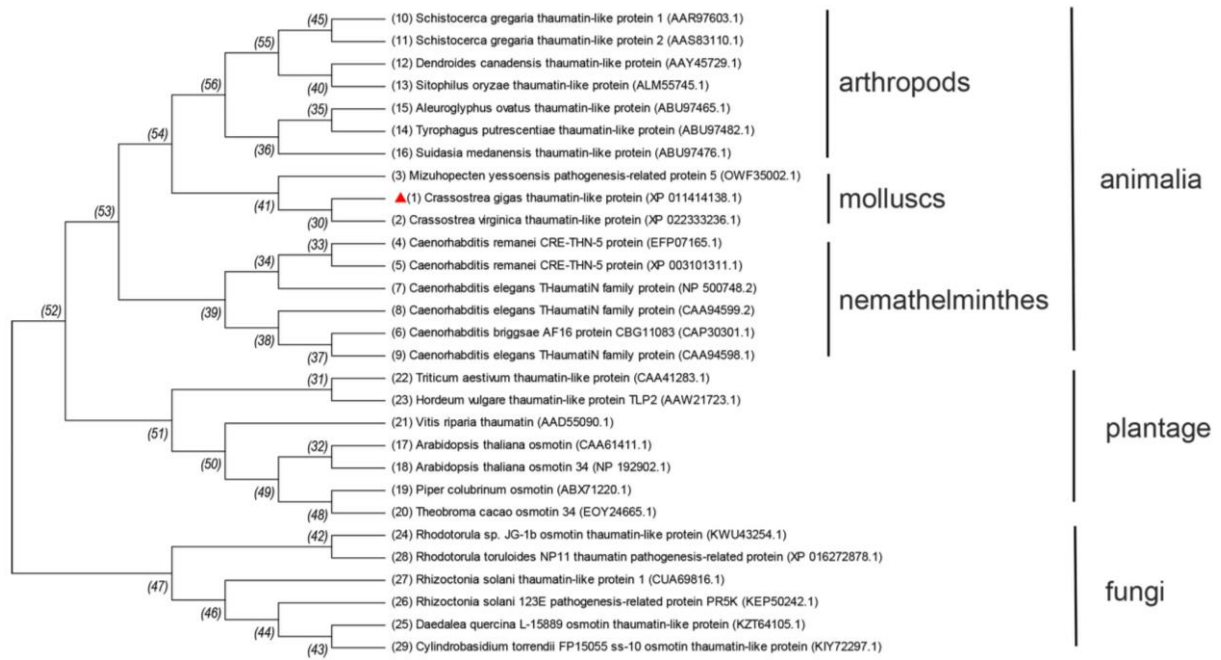
Fig. 3 The phylogenetic tree of *Cg*TLP and TLP homologues of other species. The phylogenetic tree analysis of the amino acid sequences of TLPs was constructed by the neighbor-joining method and was bootstrapped 1000 times using the MEGA 6.06 software. The *Cg*TLP was marked by a red triangle
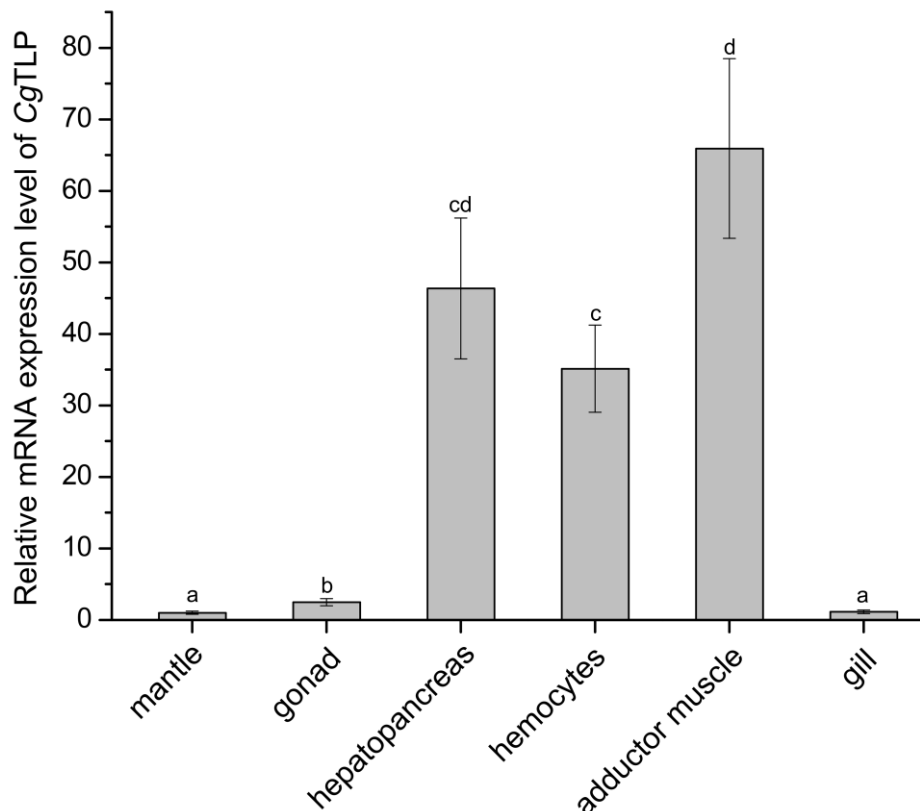

Fig. 4 The mRNA expression levels of *Cg*TLP in different tissues of adult oyster. The *Cg*EF (elongation factor) gene expression was used as an internal control and mantle sample was used as the reference sample. Each value was shown as mean ± S.D. (N = 3), and bars with different characters were significantly different ($p < 0.05$)
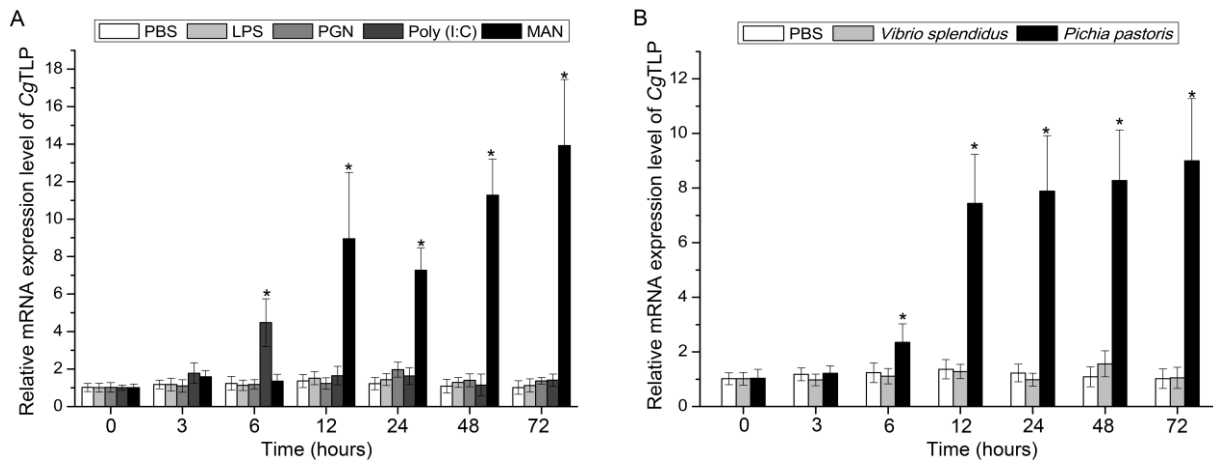
Fig. 5 The mRNA expression patterns of *Cg*TLP in hemocytes. A: Temporal mRNA expression of *Cg*TLP in hemocytes after LPS, PGN, Poly (I:C) and MAN stimulation at 0, 3, 6, 12, 24, 48, and 72 h, respectively. B: Temporal mRNA expression of *Cg*TLP in hemocytes after *V. splendidus* and *P. pastoris* stimulations at 0, 3, 6, 12, 24, 48, and 72 h, respectively. The relative expression values were shown as mean ± SD (N=3). Asterisk indicated significant difference from control ($p < 0.05$)

mice. The positive signals of FITC labeled antibody to *Cg*TLP protein were of the green fluorescence signal, which was mainly observed in the cytoplasm of the oyster hemocytes, while the nucleus of hemocytes were stained in blue fluorescence (Fig. 7).

The activity of rCgTLP to inhibit the growth of microbes

The microbe growth inhibition activity of r*Cg*TLP was assessed by detecting the microbe growth curve. Within the detection time (12 hours) and concentration range (0.000-0.500 mg/mL), there was

no obvious growth suppression activity against *S. aureus* and *V. splendidus* ($p > 0.05$) (Fig. 8A and 8B). However, the growth of *P. pastoris* in 0.250 mg/mL and 0.500 mg/mL r*Cg*TLP treatment groups was significantly suppressed ($p < 0.05$), compared with that in the blank group from 7 h to 16 h post treatment. Moreover, the growth level of *P. pastoris* in the 0.500 mg/mL r*Cg*TLP treatment group was significantly lower ($p < 0.05$) than that in the 0.250 mg/mL r*Cg*TLP treatment group during 7-16 h (Fig. 8C). The antifungal effect of r*Cg*TLP to *P. pastoris* was strengthened with the increase of protein concentration.
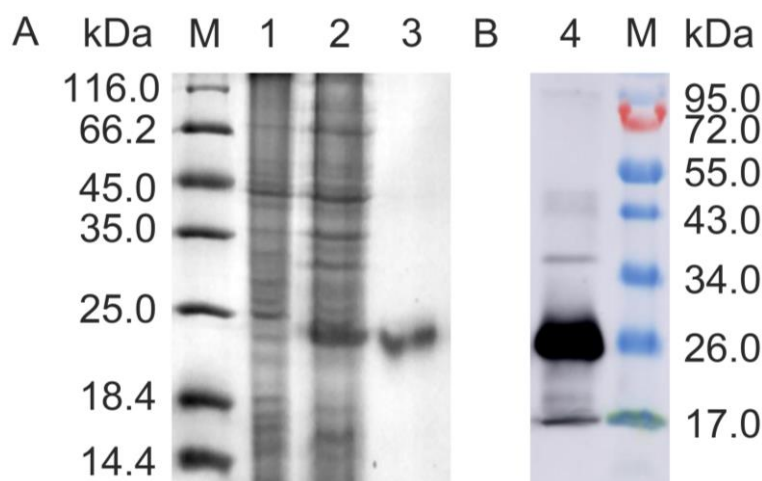
Fig. 6 SDS-PAGE and western blotting analysis of r*Cg*TLP protein. A: SDS-PAGE of r*Cg*TLP protein. M: Protein molecular standard (kDa); Lane 1: Negative control for r*Cg*TLP; Lane 2: IPTG induced r*Cg*TLP; Lane 3: Purified r*Cg*TLP. B: Western blotting of r*Cg*TLP protein. Lane 4: Western blotting of r*Cg*TLP. M: Pre-dyed protein molecular standard (kDa)
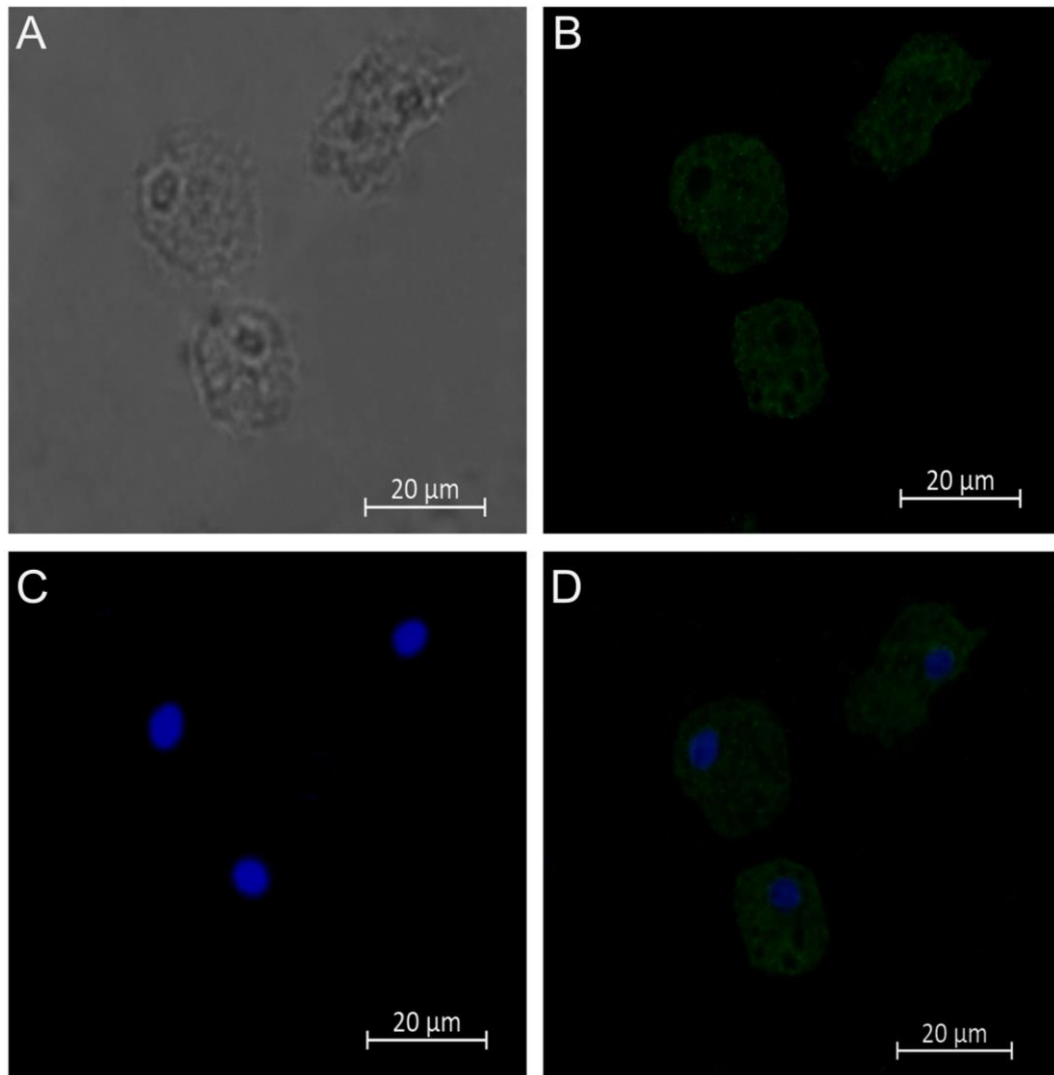
Fig. 7 Fluorescent microscopy analysis of *Cg*TLP (green) distribution in hemocytes of *C. gigas*. A: The hemocytes were observed in light field; B: The *Cg*TLP was labeled green by polyclonal antibody of *Cg*TLP and Alexa Flour 488 labeled second antibody in single section; C: The nuclei of hemocytes were stained blue by DAPI in single section; D: The merged chart. The scale bar was 20 μm

*The β-1,3-glucanase and chitinase activities of r*Cg*TLP*

In the β-1,3-glucanase activity assay, the OD_{450} of experimental group with r*Cg*TLP (0.250 mg/mL) was significantly higher (4.10-fold, $p < 0.05$) than that in control group without r*Cg*TLP (Fig. 9A). However, the OD_{585} of experimental group with r*Cg*TLP showed no significant change compared with control group in the chitinase activity assay ($p > 0.05$) (Fig. 9B).

Discussion

Thaumatin-like proteins (TLPs) have been reported to be involved in host responses against a wide range of stresses, such as pathogen/pest invasion, wounding, drought, and cold hardiness (Leone *et al.*, 2006). In this study, a homologue of

TLP with a theoretical molecular weight of 25.97 kDa was identified in oyster *C. gigas*. It was consistent with the previous reports that TLPs are about 200 amino acids (Zhang *et al.*, 2012) with the molecular weight of 21-26 kDa (Petre *et al.*, 2011). There was a THN domain in *Cg*TLP contained, which was an exclusive domain of TLP families (Leone *et al.*, 2006). The deduced amino acid sequence of *Cg*TLP shared high similarity with other known TLPs, such as the thaumatin-like protein from *C. virginica* (XP-022333236.1) and the pathogenesis-related protein 5 from *M. yessoensis* (OWF35002.1). The putative mature polypeptide of *Cg*TLP was of cysteine-rich, which was consistent with the previous report that most TLPs contained 16 conserved cysteine residues (Fierens *et al.*, 2009). These cysteine residues could be paired to form disulfide bonds, which were expected to be a relatively stable
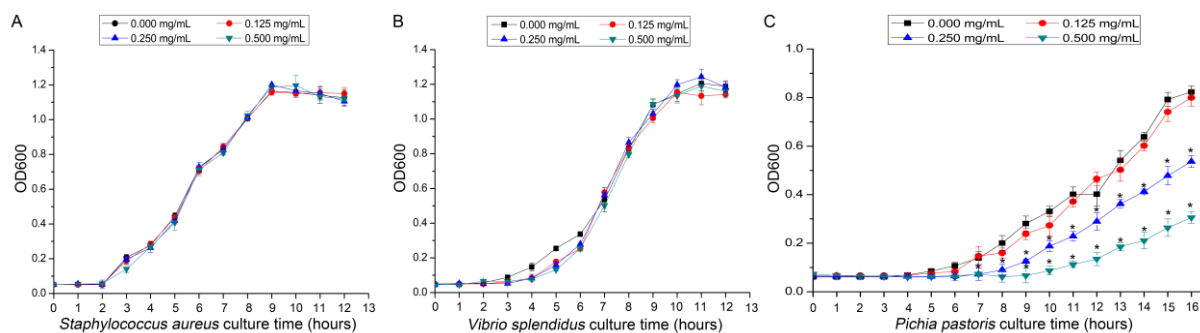
Fig. 8 The growth suppression activity of r*Cg*TLP was detected by growth curve of *S. aureus* (A), *V. splendidus* (B) and *P. pastoris* (C). Each value was shown as mean ± SD (N=3). Asterisk indicated significant difference from control ($p < 0.05$)

chemical structure to resist heat, degradation, and acid stress (Liu *et al.*, 2010). There was an N-terminal signal peptide in the putative polypeptide of *Cg*TLP contained, which could target the mature proteins into certain organelles (Anžlovar *et al.*, 2003). The three-dimensional structure of *Cg*TLP was similar to the crystal structures of plant TLPs (Ghosh *et al.*, 2008). Three domains and a cleft structure between domains Ⅰ and Ⅱ were identified in *Cg*TLP. The domain Ⅰ was formed by a β-sandwich with 11 β-sheets, which was highly conservative in TLP family members (Clustal *et al.*, 1994). The TLPs from different species possess different domain Ⅱ or domain Ⅲ, which is determined by the number of β-sheet and α-helical in domain Ⅱ or domain Ⅲ, respectively. The cleft between domain Ⅰ and Ⅱ had an acidic, neutral, or basic nature for binding different ligands/receptors (Min *et al.*, 2004). The difference of the domain Ⅲ can contribute to different enzymatic activity of TLPs (Abdin *et al.*, 2011). All these results suggested that *Cg*TLP was highly homologous to the TLPs from fungi, plants, and animals (Wang *et al.*, 2014).

A growing number of studies indicated that TLPs had antifungal function, and played an extremely important role for the organisms surviving from the environment stress (Anžlovar *et al.*, 2003). The mRNA expression of TLPs could be induced when plants were exposed to biotic and abiotic stresses (Misra *et al.*, 2018). In the present study, the mRNA transcripts of *Cg*TLP were much higher in adductor muscle, hemocytes and hepatopancreas than that in other organs of *C. gigas*. Hemocytes and hepatopancreas were the major immune organs of *C. gigas* (Wang *et al.*, 2018). Because TLPs were regarded as Immune-related genes, it was reasonable that the mRNA expression level of *Cg*TLP was high in these immune organs of *C. gigas*. Some fungi could cause oyster diseases by sticking and infecting the adductor muscle (Bower *et al.*, 1994). Meanwhile, in the present study, the antifungal activity of r*Cg*TLP was verified *in vitro*, so we speculated that the high expression of *Cg*TLP in adductor muscle might be related to its anti-fungi activity. Of course, it did not exclude that *Cg*TLP played other physiological functions in adductor

muscle (Liu *et al.*, 2010). The higher mRNA expression in these tissues indicated that *Cg*TLP might play an important role in the immune response of *C. gigas* (Wang *et al.*, 2018). In addition, significant changes of *Cg*TLP mRNA transcripts could be detected in the hemocytes after *P. pastoris* or MAN stimulation. Similarly, it was reported that TLPs could be induced by the presence of fungal molds (such as MAN, chitin, and β-1,3-glucan) and fungi *Puccinia triticina* (Zhang *et al.*, 2017). TLPs could also be induced by some kind of virus or viral simulacrum (Kinkema *et al.*, 2000). In this study, the mRNA expression of *Cg*TLP in hemocytes was up-regulated after Poly (I:C) stimulation from 3 h (1.51-fold change, $p > 0.05$) and peaked at 6 h (3.62-fold change, $p < 0.05$). These results demonstrated that the *Cg*TLP might also play an important role in the immune response to virus infection in *C. gigas*. No significant changes were observed in the mRNA expression levels of *Cg*TLP among control group, *V. splendidus* group, LPS group, and PGN group during the whole experimental process, indicating *Cg*TLP could not be induced by the presence of bacteria or the bacterial simulacrum. It was consistent with the findings that bacteria could not induce the mRNA expression of TLP in *Pinus thunbergii* (Solano *et al.*, 2013). Similar to plant TLPs, *Cg*TLP protein was mainly distributed in the cytoplasm of the oyster hemocytes, indicating that the mature *Cg*TLP might perform as cytoplasmic protein to play important roles in the innate immune response of *C. gigas* against fungal and viral infection, and resistance to stresses (Gómez-Casado *et al.*, 2014).

TLP family members have been reported to inhibit several kinds of fungi including Taphrinomycotina, Saccharomycotina, and Basidiomycota (Anžlovar *et al.*, 2003; Jung *et al.*, 2005; Hayashi *et al.*, 2014). In the present study, the antifungal and antibacterial activities of r*Cg*TLP were investigated *in vitro*. r*Cg*TLP could inhibit the growth of *P. pastoris*, which was in line with previous reports that most of plant TLPs exhibited antifungal activities (Liu *et al.*, 2010). Interestingly, r*Cg*TLP could not inhibit the growth of gram-positive bacteria, *S. aureus* and gram-negative bacteria, *V. splendidus*. Similarly,
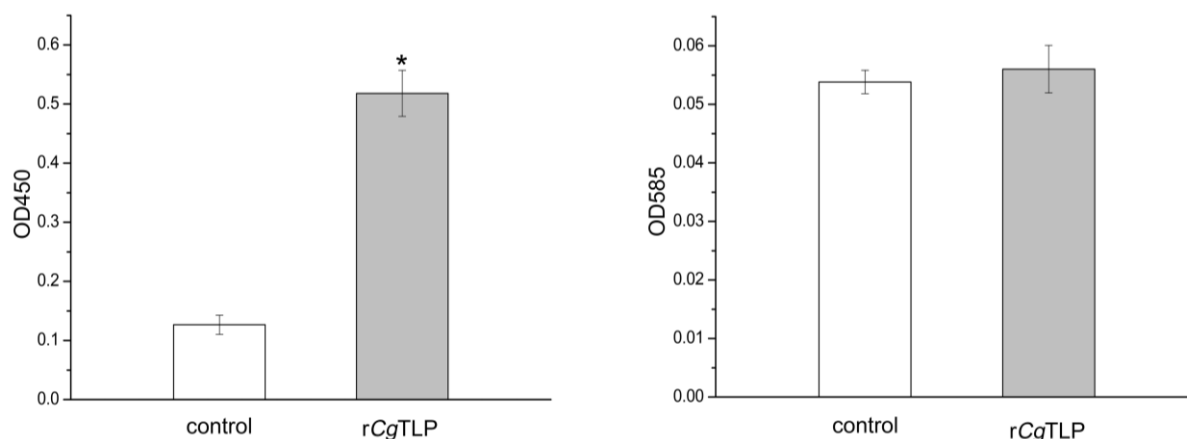
Fig. 9 The absorbance of enzyme activity detection of r*Cg*TLP. A: The absorbance of β-1,3-glucanase activity detection of r*Cg*TLP. B: The absorbance of chitinase activity detection of r*Cg*TLP. Each value was shown as mean ± SD (N=3). Asterisk indicated significant difference from control ($p < 0.05$)

some plants TLPs, such as *Oryza sativa* TLP, *A. thaliana* TLP, and *Pinus monticola* TLP, also did not display inhibitory effect on bacteria (Futamura *et al.*, 2005; Zhang *et al.*, 2007; Singh *et al.*, 2017). These results suggested that *Cg*TLP might exert selective inhibitory activity to fungi.

It has been reported that the inhibition activities of TLPs to microorganisms owe to their β-1,3-glucanase or chitinase activities (Menu-Bouaouiche *et al.*, 2003). For instance, TLP from *Musa acuminata* could hydrolyze β-1,3-glucan (Menu-Bouaouiche *et al.*, 2003), and TLP from *Picea glauca* possessed chitinase activity (Beleneva *et al.*, 2011). Some TLPs even did not possess enzymatic activity (Hernández-Blanco *et al.*, 2007; Borad *et al.*, 2008; Miura *et al.*, 2013), which exert their antifungal activities by permeabilizing cell membranes (Brandazza *et al.*, 2004; Meng *et al.*, 2017). In order to explore the possible antifungal mechanism of *Cg*TLP, the β-1,3-glucanase and chitinase activities of r*Cg*TLP were evaluated *in vitro*. r*Cg*TLP displayed obvious β-1,3-glucanase activity, but no chitinase activity, suggesting that the antifungal activity of r*Cg*TLP might be ascribed to its β-1,3-glucanase activity rather than chitinase activity. The different activities of TLPs were related to the difference of their domain Ⅱ and Ⅲ in difference species (Rep *et al.*, 2002). The domain Ⅱ and Ⅲ of *Cg*TLP were similar to the domain Ⅱ and Ⅲ of the TLP from *Musa acuminate* (Menu-Bouaouiche *et al.*, 2003), which presented β-1,3-glucanase activity. The antifungal activity of *Cg*TLP was suspected to be determined by its special domain Ⅱ and Ⅲ structure.

In summary, a novel *Cg*TLP with a classical THN domain was identified from oyster *C. gigas* for the first time. The mRNA transcripts of *Cg*TLP were highly expressed in adductor muscle, hepatopancreas and hemocytes, and could be induced by fungal stimulation rather than bacterial stimulation. r*Cg*TLP could significantly suppress the growth of *P. pastoris*, but not *S. aureus* and *V. splendidus*. The antifungal activity of r*Cg*TLP might

be ascribed to its β-1,3-glucanase activity rather than chitinase activity. This study expanded the knowledge on the functions of TLP in the antifungal immune defense system in oyster, and threw light on the evolutionary of TLPs.

References

Abdin MZ, Kiran U, Alam A. Analysis of osmotin, a PR protein as metabolic modulator in plants. Bioinformation. 5: 336-340, 2011.

Anžlovar S, Dermastia M. The comparative analysis of osmotins and osmotin-like PR-5 proteins. Plant Biol. 5: 116-124, 2003.

Blouin AG, Biccheri R, Khalifa ME, Pearson MN, Pollini CP, Hamiaux C, *et al.* Characterization of Actinidia virus 1, a new member of the family *Closteroviridae* encoding a thaumatin-like protein. Arch. Virol. 163: 229-234, 2018.

Borad V, Sriram S. Pathogenesis-related proteins for the plant protection. Asian J. exp. Sci. 22: 189-196, 2008.

Brandazza A, Angeli S, Tegoni M, Cambillau C, Pelosi P. Plant stress proteins of the thaumatin-like family discovered in animals. FEBS Lett. 572: 3-7, 2004.

Breiteneder H, Ebner C. Molecular and biochemical classification of plant-derived food allergens. J. Allergy Clin. Immunol. 106: 27-36, 2000.

Bower S, McGladdery S, Price I. Synopsis of infectious diseases and parasites of commercially exploited shellfish. Annu. Rev. Fish Dis. 4: 1-199, 1994.

Cao J, Lv Y, Hou Z, Li X, Ding L. Expansion and evolution of thaumatin-like protein (TLP) gene family in six plants. Plant Growth Regul. 22: 299-307, 2016.

Chen H, Chen Y. Diseases of cultured oysters caused by pathogenetic microbes. Fish. Sci. 26: 531-534, 2007.

Clustal W. Improving the sensitivity of progressive multiple sequence alignment through sequence weighting, position-specific gap penalties and weight matrix choice. Nucleic Acids Res. 22: 4673-4680, 1994.

Fierens E, Gebruers K, Voet ARD, Maeyer MD, Courtin CM, Delcour JA. Biochemical and structural characterization of TLXI, the *Triticum aestivum L.* thaumatin-like xylanase inhibitor. J. Enzyme Inhib. Med. Chem. 24: 646–654, 2009.

Fierens E, Rombouts S, Gebruers K, Goesaert H, Brijs K, Beaugrand J, *et al.* A novel type of xylanase inhibitor from wheat (*Triticum aestivum*) belonging to the thaumatin family. Biochem. J. 403: 583-591, 2007.

Franco OL, Rigden DJ, Melo FR, Grossidesá MF. Plant α-amylase inhibitors and their interaction with insect α-amylases. Eur. J. Biochem. 269: 397-412, 2002.

Futamura N, Tani N, Tsumura Y, Nakajima N, Sakaguchi M, Shinohara K. Characterization of genes for novel thaumatin-like proteins in *Cryptomeria japonica*. Tree Physiol. 26: 51-62, 2005.

Garcia-Casado G, Collada C, Allona I, Soto A, Casado R, Rodriguez-Cerezo E, *et al.* Characterization of an apoplastic basic thaumatin-like protein from recalcitrant chestnut seeds. Physiol. Plant. 110: 172-180, 2000.

Ghosh R, Chakrabarti C. Crystal structure analysis of NP24-I: a thaumatin-like protein. Planta. 228: 883-890, 2008.

Gómez-Casado C, Murua-García A, Garrido-Arandia M, González-Melendi P, Sánchez-Monge R, Barber D, *et al.* Alt a 1 from Alternaria interacts with PR5 thaumatin-like proteins. FEBS Lett. 588: 1501-1508, 2014.

Guo X, He Y, Zhang L, Lelong C, Jouaux A. Immune and stress responses in oysters with insights on adaptation. Fish Shellfish Immunol. 46: 107-119, 2015.

Hayashi M, Shiro S, Kanamori H, Mori-Hosokawa S, Sasaki-Yamagata H, Sayama T, *et al.* A thaumatin-like protein, Rj4, controls nodule symbiotic specificity in soybean. Plant Cell Physiol. 55: 1679-1689, 2014.

Hegde VL, Kumar A, Hassan G, Sreenath K, Hegde ML, Venkatesh YP. Identification and characterization of a basic thaumatin-like protein (TLP 2) as an allergen in sapodilla plum (*Manilkara zapota*). Mol. Nutr. Food Res. 58: 894-902, 2014.

Hernández-Blanco C, Feng DX, Hu J, Sánchez-Vallet A, Deslandes L, Llorente F, *et al.* Impairment of cellulose synthases required for Arabidopsis secondary cell wall formation enhances disease resistance. Plant Cell. 19: 890-903, 2007.

Jung YC, Lee HJ, Yum SS, Soh WY, Cho DY, Auh CK, *et al.* Drought-inducible-but ABA-independent-thaumatin-like protein from carrot (*Daucus carota L.*). Plant Cell Rep. 24: 366-373, 2005.

Kinkema M, Fan W, Dong X. Nuclear localization of NPR1 is required for activation of PR gene expression. Plant Cell. 12: 2339-2350, 2000.

Kitajima S, Sato F. Plant pathogenesis-related proteins: molecular mechanisms of gene expression and protein function. J. Biochem. 125: 1-8, 1999.

Leone P, Menu-Bouaouiche L, Peumans WJ, Payan F, Barre A, Roussel A, *et al.* Resolution of the structure of the allergenic and antifungal banana fruit thaumatinlike protein at 1.7-A. Biochimie. 88: 45-52, 2006.

Li H, Zhang H, Jiang S, Wang W, Xin L, Wang H, *et al.* A single-CRD C-type lectin from oyster *Crassostrea gigas* mediates immune recognition and pathogen elimination with a potential role in the activation of complement system. Fish Shellfish Immunol. 44: 566-575, 2015.

Liu JJ, Zamani A, Ekramoddoullah AM. Expression profiling of a complex thaumatin-like protein family in western white pine. Planta. 231: 637-651, 2010.

Liu J, Sturrock R, Ekramoddoullah AK. The superfamily of thaumatin-like proteins: its origin, evolution, and expression towards biological function. Plant Cell Rep. 29: 419-436, 2010.

Liu R, Qiu L, Yu Z, Zi J, Yue F, Wang L, *et al.* Identification and characterisation of pathogenic *Vibrio splendidus* from Yesso scallop (*Patinopecten yessoensis*) cultured in a low temperature environment. J. Invertebr. Pathol. 114: 144-150, 2013.

Livak KJ, Schmittgen TD. Analysis of relative gene expression data using real-time quantitative PCR and the $2^{-\Delta\Delta Ct}$ method. Methods. 25: 402-408, 2001.

Meng FL, Wang J, Wang X, Li YX, Zhang XY. Expression analysis of thaumatin-like proteins from *Bursaphelenchus xylophilus* and *Pinus massoniana*. Physiol. Mol. Plant Pathol. 100: 178-184, 2017.

Menu-Bouaouiche L, Vriet C, Peumans WJ, Barre A. A molecular basis for the endo-β-1,3-glucanase activity of the thaumatin-like proteins from edible fruits. Biochimie. 85:123-131, 2003.

Min K, Ha SC, Hasegawa PM, Bressan RA, Yun D-J, Kim KK. Crystal structure of osmotin, a plant antifungal protein. Proteins. 54: 170-173, 2004.

Misra RC, Kamthan M, Kumar S, Ghosh S. A thaumatin-like protein of *Ocimum basilicum* confers tolerance to fungal pathogen and abiotic stress in transgenic *Arabidopsis*. Sci. Rep. 6: 25340, 2018.

Miura K, Furumoto T. Cold signaling and cold response in plants. Int. J. Mol. Sci. 14: 5312-5337, 2013.

Noh MY, Jo YH. Identification and sequence analysis of two thaumatin-like protein (*Tm*TLP) genes from *Tenebrio molitor*. Entomol. Res. 46: 354-359, 2016.

Paillard C, Roux FL, Borrego JJ. Bacterial disease in marine bivalves, a review of recent studies: Trends and evolution Aquat. Aquat. Living Resour. 17: 477-498, 2004.

Petre B, Major I, Rouhier N, Duplessis S. Genome-wide analysis of eukaryote thaumatin like proteins (TLPs) with an emphasis on poplar. BMC Plant Biol. 11: 33, 2011.

Rep M, Dekker HL, Vossen JH, Boer ADD, Houterman PM, Speijer D, *et al.* Mass spectrometric identification of isoforms of PR proteins in xylem sap of fungus-infected tomato. Plant Physiol. 130: 4-16, 2002.

Sakamoto Y, Watanabe H, Nagai M, Nakade K, Takahashi M, Sato T. Lentinula edodes tlg1 encodes a thaumatin-like protein that is involved in lentinan degradation and fruiting body senescence. Plant Physiol. 141: 793-801, 2006.

Shatters RG, Boykin LM, Lapointe SL, Hunter WB, Rd WA. Phylogenetic and structural relationships of the PR5 gene family reveal an ancient multigene family conserved in plants and select animal taxa. J. Mol. Evol. 63: 12-29, 2006.

Singh S, Tripathi RK, Lemaux PG, Buchanan BB, Singh J. Redox-dependent interaction between thaumatin-like protein and β-glucan influences malting quality of barley. Proc. Natl. Acad. Sci. U.S.A. 7: 201701824, 2017.

Solano R, Gimenez-Ibanez S. Nuclear jasmonate and salicylate signaling and crosstalk in defense against pathogens. Front. Plant Sci. 4: 72, 2013.

Sun Y, Zhou Z, Wang L, Yang C, Jianga S, Song L. The immunomodulation of a novel tumor necrosis factor (*Cg*TNF-1) in oyster *Crassostrea gigas*. Dev. Comp. Immunol. 45: 291-299, 2014.

Wang L, Li L, Zhang Y, Guo Z, Wang Y, Yang G, *et al.* Characterization of *LhSor*PR5, a Thaumatin-like Protein from the *Oriental Hybrid Lily Sorbonne*. Int. J. Agric. Biol. 19: 865-872, 2017.

Wang L, Song X, Song L. The oyster immunity. Dev. Comp. Immunol. 80: 99-118, 2018.

Wang J, Han S, Li YX, Deng X, Zhang XY. Cloning of TLP-1 gene and prediction of TLP-1 protein structure of *Bursaphelenchus xylophilus*. J. Sichuan Agric. Univ. 32: 6, 2014.

Yang C, Gao Q, Liu C, Wang L, Zhou Z, Gong C, *et al.* The transcriptional response of the Pacific oyster *Crassostrea gigas* against acute heat stress. Fish Shellfish Immunol. 68: 132-143, 2017.

Yasmin N, Saleem M, Naz M, Gul R, Rehman HM. Molecular characterization, structural modeling, and evaluation of antimicrobial activity of basrai Thaumatin-Like protein against fungal infection. Biomed Res. Int. 2017: 9, 2017.

Zhang G, Fang X, Guo X, Li L, Xu F, Yang P, *et al.* The oyster genome reveals stress adaptation and complexity of shell formation. Nature. 490: 49-54, 2012.

Zhang T, Qiu L, Sun Z, Wang L, Zhou Z, Liu R, *et al.* The specifically enhanced cellular immune responses in Pacific oyster (*Crassostrea gigas*) against secondary challenge with *Vibrio splendidus*. Dev. Comp. Immunol. 45: 141-150, 2014.

Zhang Y, Shih DS. Isolation of an osmotin-like protein gene from strawberry and analysis of the response of this gene to abiotic stresses. J. Plant Physiol. 164: 68-77, 2007.

Zhang Y, Yan H, Wei X, Zhang J, Wang H, Liu D. Expression analysis and functional characterization of a pathogen-induced thaumatin-like gene in wheat conferring enhanced resistance to *Puccinia triticina*. J. Plant Interact. 12: 332-339, 2017.